Journal of Medicinal Chemistry

Subscriber access provided by CORNELL UNIVERSITY LIBRARY

Article

Optimization of Platelet Derived Growth Factor Receptor (PDGFR) inhibitors for duration of action, as an inhaled therapy for lung remodeling in pulmonary arterial hypertension

Duncan E. Shaw, Ferheen Baig, Ian Bruce, Sylvie Chamoin, Stephen P. Collingwood, Sarah Cross, Satish Dayal, Peter Drueckes, Pascal Furet, Vikki Furminger, Deborah Haggart, Martin Hussey, Irena Konstantinova, Jon C. Loren, Valentina Molteni, Sonia Roberts, John Reilly, Alex M Saunders, Rowan Stringer, Lilya Sviridenko, Matthew Thomas, Christopher G Thomson, Christine Tomlins, Ben Wen, Vince Yeh, and Andrew Pearce

J. Med. Chem., **Just Accepted Manuscript** • DOI: 10.1021/acs.jmedchem.6b00703 • Publication Date (Web): 09 Aug 2016

Downloaded from http://pubs.acs.org on August 9, 2016

Just Accepted

"Just Accepted" manuscripts have been peer-reviewed and accepted for publication. They are posted online prior to technical editing, formatting for publication and author proofing. The American Chemical Society provides "Just Accepted" as a free service to the research community to expedite the dissemination of scientific material as soon as possible after acceptance. "Just Accepted" manuscripts appear in full in PDF format accompanied by an HTML abstract. "Just Accepted" manuscripts have been fully peer reviewed, but should not be considered the official version of record. They are accessible to all readers and citable by the Digital Object Identifier (DOI®). "Just Accepted" is an optional service offered to authors. Therefore, the "Just Accepted" Web site may not include all articles that will be published in the journal. After a manuscript is technically edited and formatted, it will be removed from the "Just Accepted" Web site and published as an ASAP article. Note that technical editing may introduce minor changes to the manuscript text and/or graphics which could affect content, and all legal disclaimers and ethical guidelines that apply to the journal pertain. ACS cannot be held responsible for errors or consequences arising from the use of information contained in these "Just Accepted" manuscripts.

ACS Publications

Journal of Medicinal Chemistry is published by the American Chemical Society. 1155 Sixteenth Street N.W., Washington, DC 20036

Published by American Chemical Society. Copyright © American Chemical Society. However, no copyright claim is made to original U.S. Government works, or works produced by employees of any Commonwealth realm Crown government in the course of their duties.

Optimization of Platelet Derived Growth Factor Receptor (PDGFR) inhibitors for duration of action, as an inhaled therapy for lung remodeling in pulmonary arterial hypertension

Duncan E. Shaw,[*^] Ferheen Baig,[+] Ian Bruce,[§] Sylvie Chamoin,[>] Stephen P. Collingwood,[§] Sarah Cross, [^] Satish Dayal,[+] Peter Drückes,[>] Pascal Furet,[>] Vikki Furminger,[§] Deborah Haggart,[»] Martin Hussey,[#] Irena Konstantinova,[#] Jon C Loren,[»] Valentina Molteni,[»] Sonia Roberts,[#] John Reilly, [§] Alex M. Saunders,[§] Rowan Stringer,[+] Lilya Sviridenko,[§] Matthew Thomas, [#] Christopher G. Thomson,[^] Christine Tomlins,[#] Ben Wen, [»] Vince Yeh,[»] and Andrew Pearce[#]

[^]Novartis Institutes of Biomedical Research(NIBR), 100 Technology Square, Cambridge MA 02139, USA; [+]Metabolism and Pharmacokinetics, [§]Global Discovery Chemistry, [#]Respiratory Diseases, NIBR Horsham, Wimblehurst Road, Horsham, West Sussex, UK; [>]NIBR Basel Fabrikstrasse 2, 4056 Basel, Switzerland; [»]Genomics Institute of the Novartis Research Foundation, 10675 John Jay Hopkins Drive, San Diego, CA 92121 USA

ABSTRACT: A series of potent PDGFR inhibitors has been identified. The series was optimized for duration of action in the lung. A novel kinase occupancy assay was used to directly measure target occupancy after *it* dosing. Compound **25** shows 24 hour occupancy of the PDGFR kinase domain, after a single *it* dose and has efficacy at 0.03 mg/kg, in the rat moncrotaline model of pulmonary arterial hypertension. Examination of PK/PD data from the optimization effort has revealed *in vitro*: *in vivo* correlations which link duration of action *in vivo* with low permeability and high basicity, and demonstrate that nonspecific binding to lung tissue increases with lipophilicity.

INTRODUCTION

Pulmonary arterial hypertension (PAH) is a progressive and deadly disease with a poor prognosis despite the introduction of multiple therapeutic classes over the last decade.[1] The disease is characterized by increases in pulmonary vascular resistance (PVR) such that the resting mean pulmonary arterial pressure rises above 25 mmHg.[2] The disease is driven by aberrant smooth muscle proliferation in the pulmonary arteries and arterioles which increasingly makes passage of blood more difficult. Characteristic plexiform lesions, which show medial hypertrophy and fibrotic intimal lesions can envelop the entire artery wall, are also features of the pathology. The current marketed therapies function by vasodilation and have limited effects on the progression of the smooth muscle proliferation or on lesion formation.[3]

The platelet derived growth factor (PDGF) is a powerful mitogen which signals through the receptor tyrosine kinases (PDGFRα and PDGFRβ). Both the chemokine and its receptor have been shown to be overexpressed in both the pulmonary artery smooth muscle cells (PASMC) and the endothelial cells of severe PAH patients. Actively proliferating PASMC have been shown to have raised levels of phosphorylated PDGFR.[4]

Oral Imatinib **1** demonstrated efficacy in the first trial to investigate the effects of a non-vasodilatory agent in PAH. The rationale for initiating the clinical trial was the activity of **1** as an inhibitor of PDGFR receptor tyrosine kinases. The drug targeted the remodeling of the pulmonary arteries and thus attempted to alter the course of the disease. Patients in the trial showed improvements in six minute walk distance and reduced PVR measured by right heart catheterisation.[5] The systemic administration of **1** is however associated with side effects and these led to significant numbers of patients withdrawing from the trial. Indeed in the IMPRES (phase III) trial, despite clear clinical benefits, a positive risk benefit ratio could not be demonstrated.[6]

It was hypothesized that an inhibitor of PDGFR locally administered by inhalation might achieve efficacy similar or better than **1** but with greatly reduced systemic side effects.

When the desired site of action is in the lung, inhalation can be used to reduce the systemic side effects of a medication. A key challenge to this approach is the rapid absorption of small molecules from the airways into the systemic circulation, since it has been clearly demonstrated that the lung offers little barrier to the absorption of soluble drugs.[7] The maintenance of duration of action in the lung such that clinical dosing can be once or twice a day is a key objective in inhaled drug design.[7]

The selective inhibition of PDGFR in the lung vasculature presented a challenging objective. Whilst there is extensive precedent for inhaled medicines demonstrating an enhanced therapeutic index, the site of action for these drugs is typically in the airway epithelial tissue (e.g. β2 agonists, M3 antagonists).[8] The target tissue for this project was the smooth muscle surrounding the pulmonary arteries and arterioles of the lung and, by definition this tissue is separated by only a short distance from the circulatory system. This presented a novel drug delivery challenge, to achieve sufficient exposure in the target tissue whilst avoiding rapid equilibration of the drug with the rest of body. Given the novel nature of the drug delivery challenge, the characteristics shown to be desirable for traditional inhaled drugs were not necessarily relevant to this project. The strategy taken was to profile a selection of potent PDGFR inhibitors in an *in vivo* mechanistic assay to measure duration of action, and in parallel to assess an extensive range of *in vitro* parameters. This data set allowed the establishment of *in vitro*: *in vivo* correlations which were then used to prioritize subsequent optimized molecules for *in vivo* testing.

A search for novel chemotypes, which could display similar kinase activity, was initiated, in the Novartis sample collection, based on the co-crystal structure of **1** with cKit (PDB: IT46)[9]. The imidazo [1, 2-*a*] pyridine **2** (Rat A10 IC_{50} 36± 16 nM) was identified as a potent inhibitor of PDGFR and cKit. Furthermore the pyrazolo [1, 5-*a*] pyridine **3** (Rat A10 IC_{50} 12± 5 nM) offered an attractive alternative chemotype (Figure 1). These molecules compared well to **1** (Rat A10 IC_{50} 162± 39 nM) in a cell based assay of PDGFβ driven proliferation in rat A10 PASMC, and thus offered attractive starting points. Compounds **2** and **3** were both identified by separate Novartis project teams in search of novel and

patentable analogues of **1**. They were considered ideal starting points for this work since they maintained a kinase selectivity profile similar to that of **1**.

Figure 1 Lead molecules identified from the Novartis sample collection

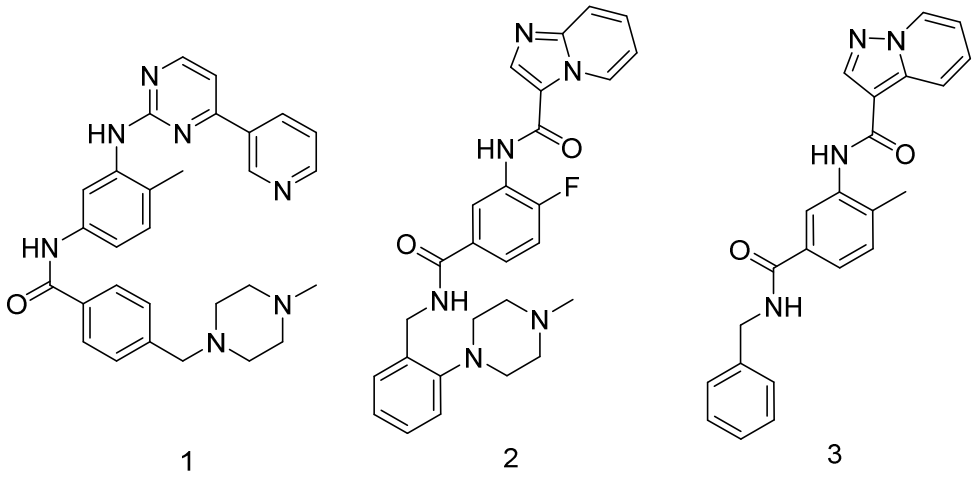

CHEMISTRY

Compounds described in this paper were synthesized according to the general scheme (Figure 2)[10]

Figure 2 General scheme for preparation of the compounds described: for specific structures of R^1 and R^2 refer to Tables 1 and 2

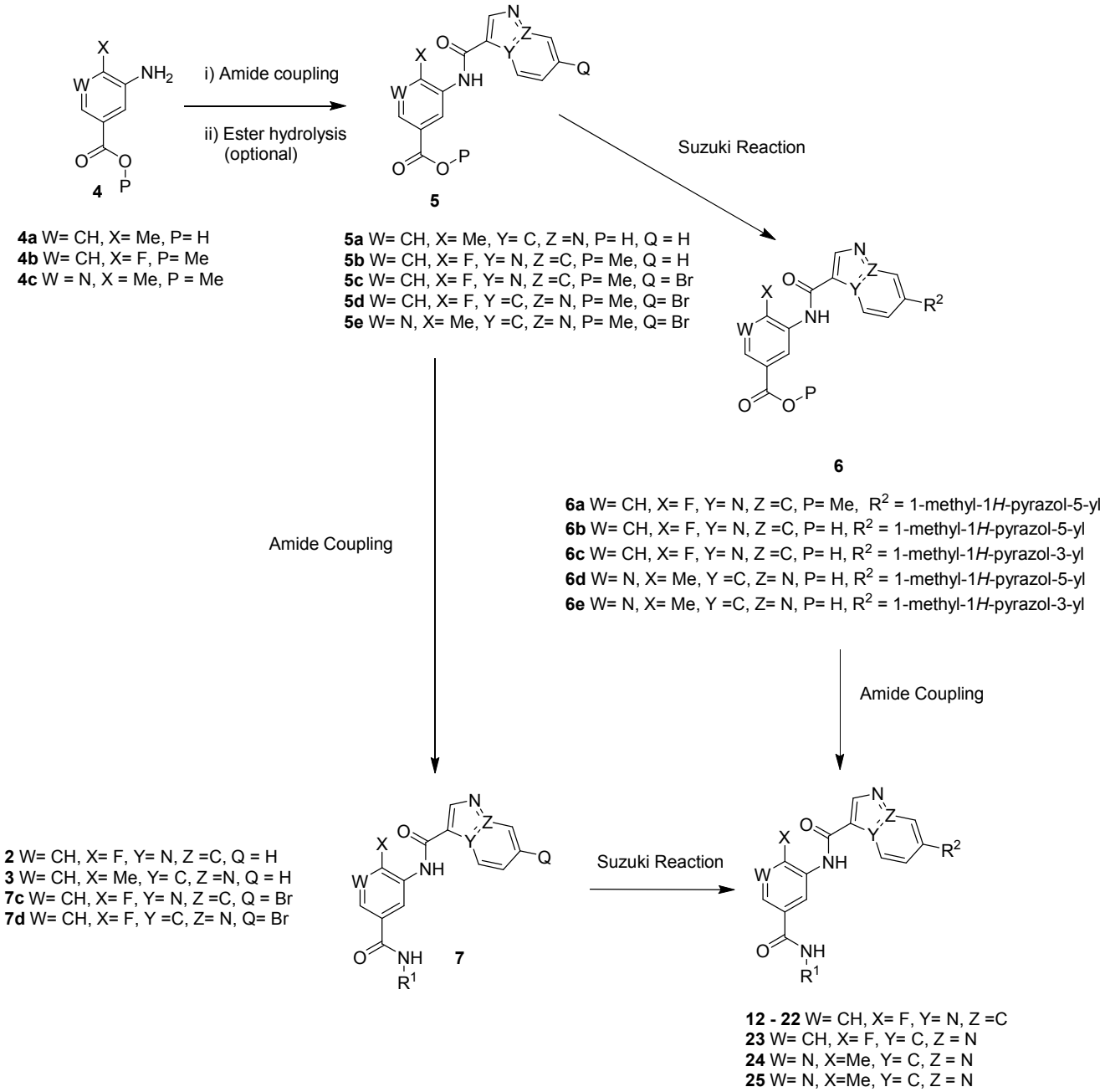

The compounds could be prepared by standard methods in a flexible way using orthogonal chemistry which allowed for a number of interchangeable synthetic routes. Largely commercially available 3-aminobenzoic acids or esters **4** were used as the core and amide coupling with fused pyrazolopyridine or imidazopyridine carboxylic acids (optionally substituted with bromine) allowed access to the central

intermediates **5.** The final compounds could then be accessed by carrying out an initial palladium catalyzed coupling to give **6**, followed by an amide coupling. Alternatively one can perform an amide coupling reaction to give **7** and then a palladium catalyzed cross coupling reaction to give the final products. This chemistry was employed flexibly to enable structural variation at either end of the molecule.

The pyridine core molecule **4c** was novel and was synthesized as described in Figure 3. Chlorination of the nitro derivative **8** allowed formation of the chloropyridine with concomitant esterification of the carboxylic acid to furnish **9**. Hydrogenation of the nitro group then allowed the core amino pyridine **4c** to be synthesized.

Figure 3 Preparation of the pyridine core

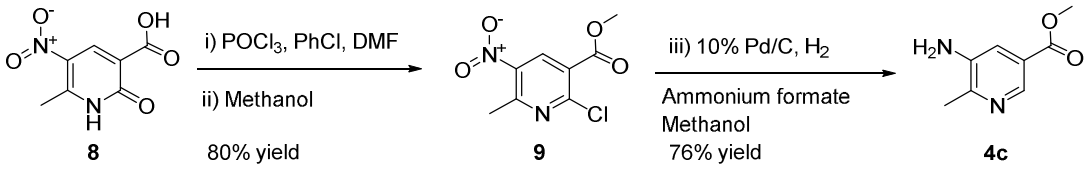

The amine groups used to form R^1 were commercially available with the exception of (5, 5-dimethyltetrahydrofuran-2-yl) methanamine **11** which was synthesized as shown in Figure 4. The commercially available bromocyclisation product **10** was converted into the intermediate azide, which was subsequently reduced using triphenylphosphine to give the desired primary amine.

Figure 4 Synthesis of (5, 5-dimethyltetrahydrofuran-2-yl) methanamine

RESULTS AND DISCUSSION

PDGFRα inhibition was assessed in a biochemical assay using the isolated kinase domain and examining the degree of phosphorylation of a probe peptide substrate in the presence of the test molecule.[11] The cell based activity of the test molecules was determined by measuring the effect of the compound on the PDGFβ driven proliferation of Rat A10 (PASMC) over a four day period. [12] A homology model was generated based on the the cKIT co-crystal structure of **1**[9] and this model was used to predict the binding mode of 7c . Examination of the predicted docking modes suggested substitution of the imidazopyridine ring of **2** at the 6-position would be tolerated since space existed at that position (Figure 5). Indeed a boost in potency was achieved when a range of small heterocycles were incorporated at this position (Table 1). The introduction of a 3-pyridyl substituent **12** gave an increase in cell based activity. The methyl 5-pyrazolyl **13** and methyl 3-pyrazolyl **14** substituents were also particularly beneficial, with reductions in permeability leading to a bigger disconnect between potency in the isolated enzyme system and that seen in the cell based assay. However, by finding successively more potent inhibitors in the enzyme assay, the desired level of cell based potency could be maintained, despite the reduced permeability. The 3-pyrazolyl substituent **15** maintained functional activity at the enzyme but was slightly less potent in the cell based assay suggesting that the reduction in permeability had begun to impact cell penetration (Table 1).

Figure 5 Docking of **7c** into the homology model generated from the PDB structure 1T46 (**1** co-crystallized with cKit)[9] A) Showing the position of **1** (cyan) compared to the proposed binding mode for **7c** (orange). B) Showing the potential space at the 6-position of the imidazopyridine, by replacement of the bromo substituent.

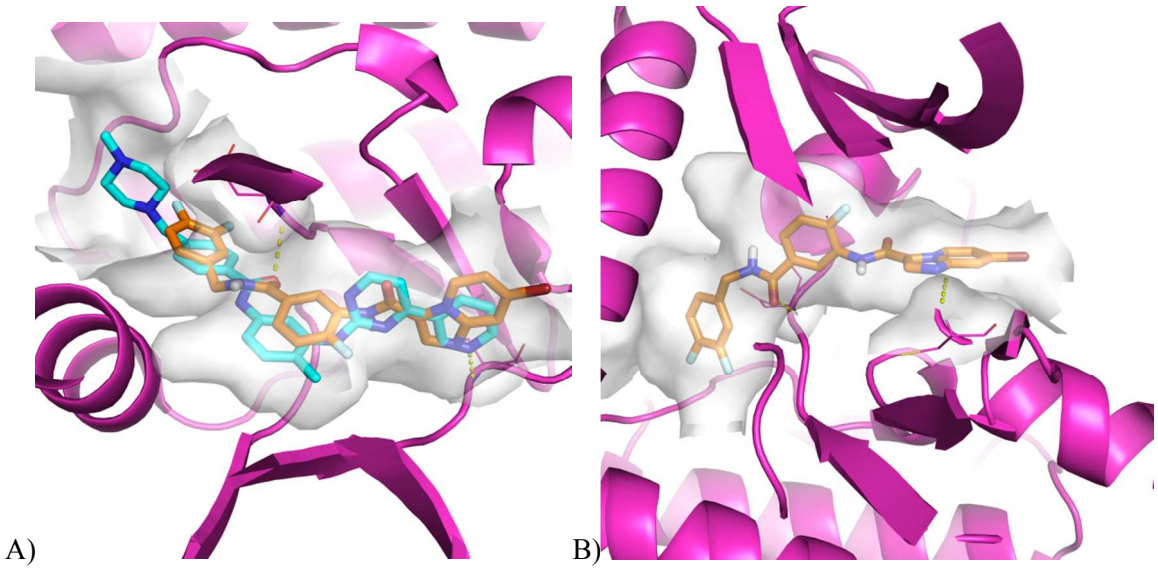

Table 1 Effect of imidazopyridine 6-substituent upon potency, permeability and lipophilicity

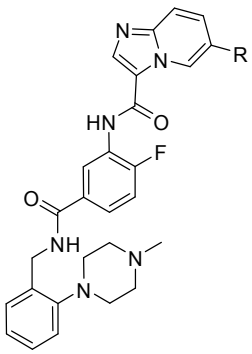

	R	CE PDGFRα IC_{50} nM[a]	Rat A10 assay IC_{50} nM[b]	PAMPA Permeability % transcellular[13]	cLog P
2	H	13±18	36±16	83.1	3.36
12		0.75±0.45	7.9±3.8	23	3.75

13		0.18±0.02	9.2±1.6	4.8	3.57
14	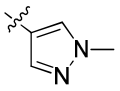	0.32±0.17	3.6±0.7	26.3	3.36
15	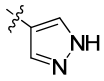	<0.1±0.01	18.7±6.9	0	3.34

a) Inhibition of probe substrate phosphorylation by PDGFRα, measured by capillary electrophoresis. Determinations based on n= 3 or more[11]

b) Inhibition of PDGFRβ driven proliferation of Rat A10 cells. Determinations based on n= >3 or more[12]

The presence of an aryl piperazine substituent in these molecules was seen as a risk in terms of potential off target activity, since compounds containing this moiety are known to bind promiscuously to GPCRs and ion channels.[14] Indeed compound **13** showed an IC_{50} of binding <10 μM at 9 out 26 GPCRs tested and exhibited binding at the HERG channel (IC_{50} = 4 μM). A search for an alternative amide substituent with a lower lipophilicity, and MW was initiated guided by docking studies (Table 2).

The substituted difluorobenzyl compound **16** showed very high potency indicating that the size of the amide substituent could be reduced without detrimental effects on potency. Compound **16** however, showed poor solubility (no detectable solubility in the i.t. dosing vehicle 10% PEG 200 / 95 % D5W) suggesting it would be beneficial to introduce polarity into the molecules. The dimethyltetrahydrofuran **17**, exhibited potency equivalent to **16** with reduced lipophilicity. The introduction of a basic amine such as **18** was also tolerated. An improved understanding of the required elements for optimal lipophilic binding was derived from comparison of compounds **19** and **20** in which no further advantage is gained by extension of the aliphatic side chains. This improved understanding led to the discovery of the cyclic derivative **21**. The potency could be improved further using the methyl 5-pyrazolyl substituent to give **22**.

Table 2 Effect of amide substituent upon potency, permeability and lipophilicity

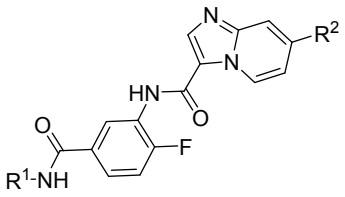

	R^1	R^2	CE PDGFRα IC_{50} nM[a]	Rat A10 assay IC_{50} nM[b]	PAMPA Permeability % transcellular[12]	cLog P
16	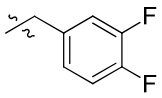	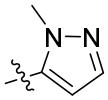	0.09±0.03	3.0±0.2	11	3.77
17	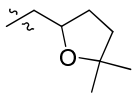	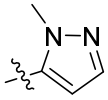	0.53±0.18	2.7 ± 0.7	81	3.26
18	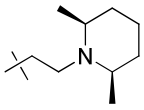	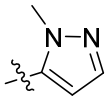	1.3±0.7	8.7± 0.8	5.4	3.19
19	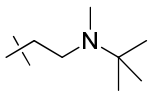	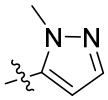	3.2±1.5	23±7	0	3.23
20	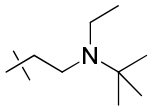	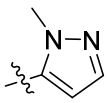	1.6±0.9	22±12	23	3.76
21	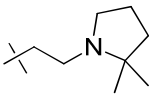	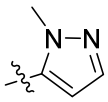	1.3±0.03	9.5±3.7	0.6	3.67

22	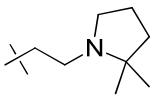	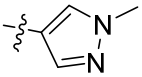	0.19±0.06	1.7±0.7	0.7	3.46

a) Inhibition of probe substrate phosphorylation by PDGFRα, measured by capillary electrophoresis. Determinations based on n= 3 or more[11]

b) Inhibition of PDGFRβ driven proliferation of Rat A10 cells. Determinations based on n= >3 or more[12]

With the SAR established for both the amide portion and the hinge binding extension, it was considered important to re-examine the alternative core structures. Both the pyrazolopyridine **23** and the 2-methylpyridine **24** showed good *in vitro* potency and allowed the direct comparison to the original imidazo[1, 2-*a*] pyridine core structure **13** (Table 3). The core changes were well tolerated in terms of potency *in vitro* and led to modified properties allowing us to examine the effects of such changes on duration of action *in vivo* (Table 4). The optimal amide and hinge extension substituents identified in the earlier work were then transferred into the 2-methylpyridine core, using the pyrazolopyridine as the hinge binding group; this allowed the identification of **25**. This compound showed a much improved selectivity profile with respect to binding to GPCRs (26 tested 24 >30 μM, M1 IC_{50} 5.0 μM; H3 IC_{50} 5.0 μM) and had an IC_{50} >30 μM at the HERG channel. These data were supportive of further profiling particularly given the low anticipated dose based on the inhaled route of delivery (Table 3)

Table 3 Effect of changes to the aniline core and the 6,5 heterocycle upon potency, permeability and lipophilicity

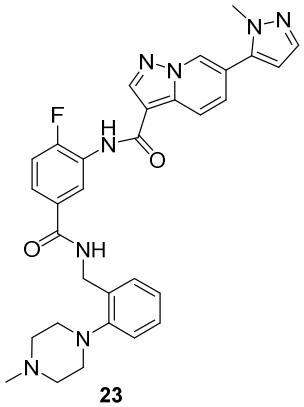

23

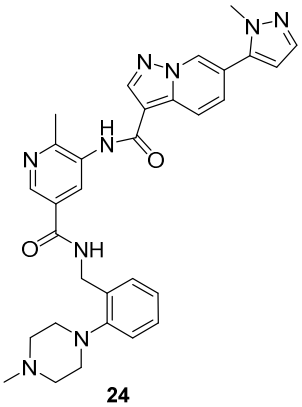

24

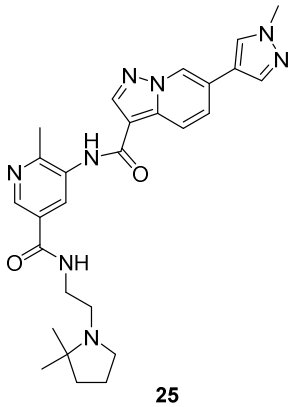

25

Compound	CE PDGFRα IC_{50} nM[a]	Rat A10 assay IC_{50} nM[b]	PAMPA Permeability % transcellular[12]	cLog P
13	0.18±0.02	9.2±1.6	4.8	3.57
23	1.2±0.8	10.3±2.8	70	3.03
24	0.96±0.5	35±12	17	3.01
25	0.2±0.08	12.8 ± 0.9	4.7	2.90

a) Inhibition of probe substrate phosphorylation by PDGFRα, measured by capillary electrophoresis. Determinations based on n= 3 or more[11]

b) Inhibition of PDGFRβ driven proliferation of Rat A10 cells. Determinations based on n= >3 or more[12]

The identified compounds were screened in a range of *in vitro* assays (High Throughput Solubility, PAMPA[13], CACO2 (A-B/B-A), CACO2 P_{app}, RLM Cl_{int}, CHI-IAM membrane retention[15], RSA binding[16], HSA binding[16], V_{ss} calc[16]) and *in silico* calculations (cLogP, PSA, cLogD) to assess their physicochemical properties (Full data set is in the supplementary information).[18] The intention of this exercise was initially to facilitate the development *of in vitro: in vivo* correlations (ivivc) rather than to screen out any particular property at this stage. Potent compounds with a range of properties were then screened *in vivo* by measurement of kinase site occupancy.

Critical to the success of this strategy was the identification of a direct method for measurement of duration of action. In this respect the identification of the PDGFR-β antibody CST4564[19] was vital. This

antibody has the remarkable property that it can only recognize PDGFR-β in its active form. When the kinase is in an inactive form (*i.e.* in the presence of a type II kinase inhibitor) the antibody does not recognize PDGFR-β in immunoprecipitation experiments. Applying this finding to ex-vivo tissue from PK-PD experiments allowed us to determine the percentage of the PDGFR-β in the given tissue sample which was bound to compound, and therefore to directly measure kinase occupancy. Control experiments were able to show that addition of excess test compound to the lysates during the processing and immunoprecipitation work up did not affect the level of PDGFR occupancy measured. This finding confirmed that our readout was directly correlated to the occupancy seen in the *in vivo* experiment.[17]

The poorly soluble analogue **16** was shown to exhibit low occupancy at 7 h after a 1 mg/kg dose, despite very high measured lung levels. This observation indicated that the drug was very likely to be still in the airway and not absorbing into the lung tissue itself. As a result of this early finding, *in vivo* testing was confined to molecules which could be shown to have sufficient solubility in the dosing vehicle (10% PEG 200 / 95 % D5W).

The dosing of soluble compounds led to much lower apparent lung levels, but also led to superior occupancy, compounds **13** and **18** for example exhibited duration of action to 7h. (Table 4)

Another key comparison was that between the core structures, with **23** showing relatively poor duration of action compared to **13**. The duration of action was recovered when the pyridyl core was introduced in **24**.

The common factor between **13** and **24** is that they possess two basic centers at physiological pH which is not the case for **23**. This suggested that these dibasic compounds had some intrinsic advantage. Additionally the decreased lipophilicity of **24** is a factor and an improved occupancy was demonstrated despite somewhat lower cell based activity.

The improved amide substituent and the optimal hinge extension, when combined with the more polar core structure **25** further improved the *in vivo* profile leading to occupancy of >80% at 24 hours after a 0.1 mg/kg dose.

Table 4 Occupancy of the PDGFR kinase domain and lung concentrations from in vivo studies

Compound	Solubility[a] mg/mL	*it* dose mg/kg	% Occ 7 h[b]	[Lung] at 7h (nM)	% Occ 24h[b]	[Lung] at 24 h (nM)
16	<0.01	1	27±11	276200±143700		
13	0.77	0.1	54±24	188±32		
13	0.77	0.4	70±25	687±188	9±19	60±39
18	0.59	0.1	75±13	302±56	0	44±16
22	> 1	0.1	82±8	1026±255	51±9	420±85
23	> 1	0.4	29±22	221±144		
24	> 1	0.4	83±8	3950±1100		
25	> 1	0.1	88±10	1304±230	81±9	680±121

a) 10% PEG200/95% D5W. i.t. dosing vehicle , i.t. dosing of vehicles with higher organic content is not well tolerated

b) As determined by immunoprecipitation from lung tissue lysates using CST4564

For a set of 40 compounds tested *in vivo*[18] a data set was obtained that enabled assessment of *in vitro*: *in vivo* correlations. The compound set consisted of potent compounds (IC_{50} < 50 nM in the rat A10 assay) all of which had good solubility in the dosing vehicle. These restrictions mean that the data set is not well suited to assessing the effect of potency or solubility upon duration of action.

As an initial unbiased approach, a random forest plot was generated to show which of the *in vitro* parameters measured correlated most strongly to occupancy at 8 h, and to the concentration of drug required to reach 50% occupancy (Occ_{50}) in the *in vivo* studies (Figure 6).

When considering occupancy at 8 hours, by far the strongest correlation was that seen to permeability in the artificial membrane PAMPA assay (x. transcellular). A correlation was also observed to clearance in rat liver microsomes (Cl_{int}, RLM.ER), and a role for basicity was identified by correlations seen to calculated Log D and pKa. Lipophilicity in isolation was not a good predictor of duration of action, but had by far the strongest correlation to Occ_{50}.

Figure 6 Random forest comparison of *in vivo* occupancy to *in vitro* parameters

A) Relative correlation strength between Occupancy at 8 hours and various i*n vitro* measurements

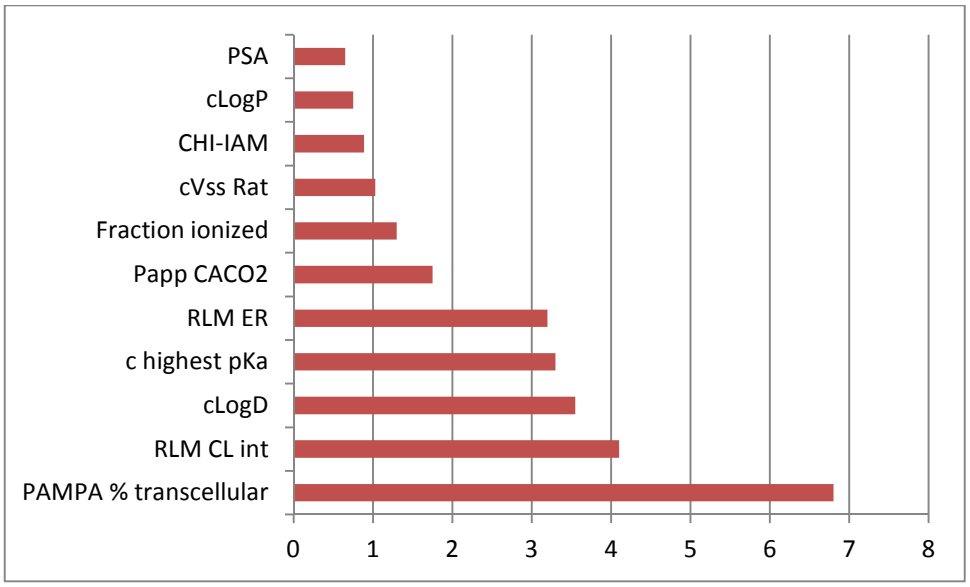

B) Relative correlation strength between Occ_{50} and various i*n vitro* measurements

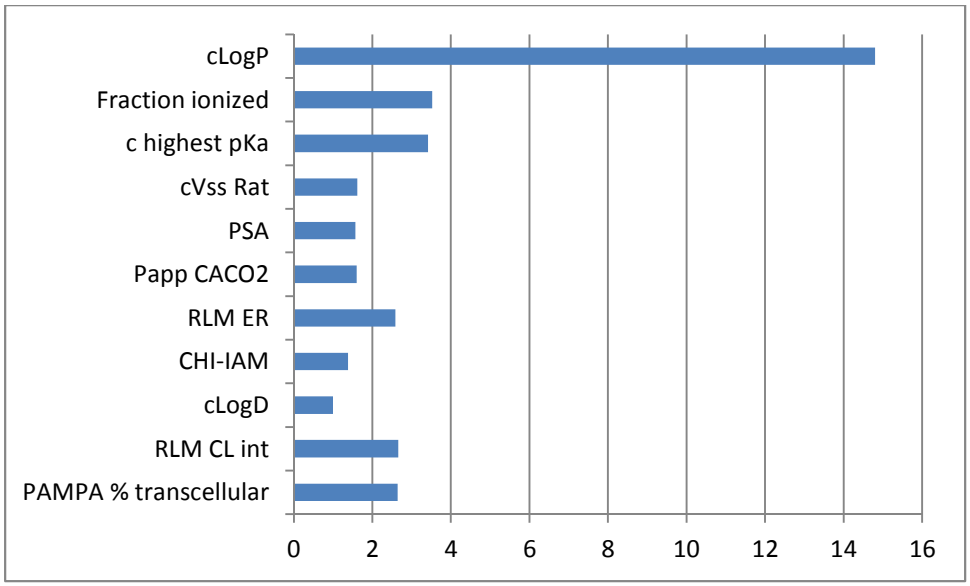

It was possible to show that permeability, measured in the artificial membrane PAMPA assay, correlated with duration of action (see Figure 7). Compounds with good occupancy at 7 hours after an *it* dose were shown to exhibit much lower permeability than those without occupancy at 7 hours ($p = 0.00003$).

Figure 7 Permeability is a key factor in determining duration of action

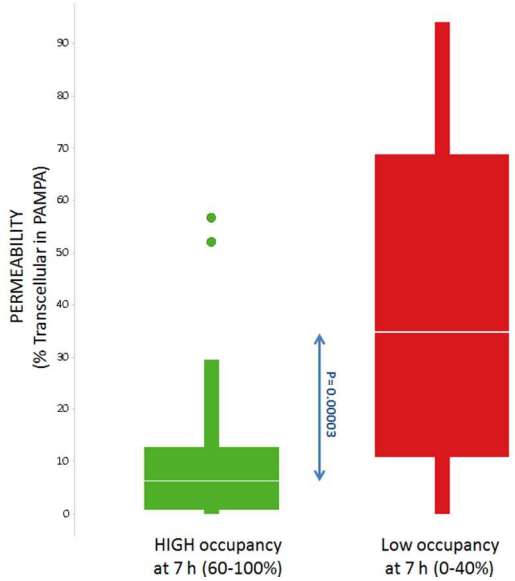

Figure 8 More basic compounds exhibit longer duration of action

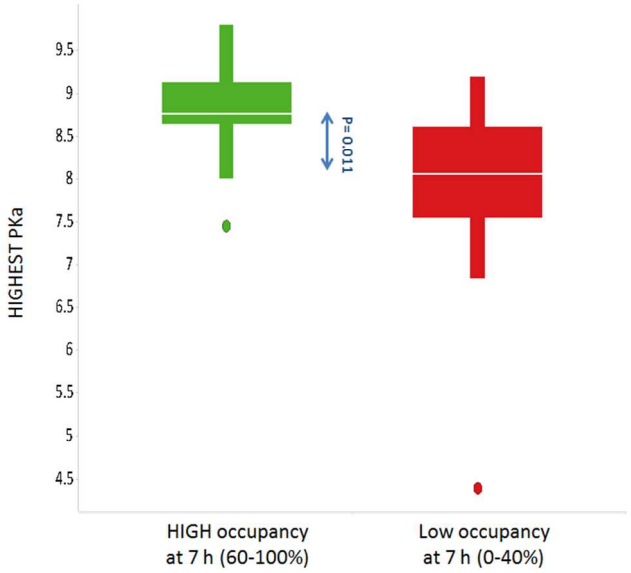

Whilst low permeability was necessary for duration of action, it was not sufficient and compounds with low permeability were also shown to lack duration of action in many cases. Absorption of low molecular weight compounds from the airway into the systemic circulation is known to be rapid.[7] One can speculate that for soluble compounds, absorption from the airway may be too rapid to allow a significant depoting effect to occur as part of the first pass absorption event. Low permeability may be necessary to slow the absorption and allow the opportunity for depoting to occur in the case where a compound has sufficient affinity for lung tissue.

A correlation with high pKa was observed, with more basic compounds showing a higher tendency to have good duration of action ($p = 0.011$) (Figure 8). This empirical observation is consistent with the known affinity of basic molecules for tissue and in this case could be a representative surrogate measure of lung tissue affinity.

Correlations were also observed within the data, when the amount of drug required to achieve 50% Occupancy (Occ_{50}) was considered. A clear positive correlation between Occ_{50} and cLogP was observed

(p = 0.00028) (Figure 9) suggesting a role for non-specific binding of drug to the tissue. Less lipophilic molecules are likely to be more available to the target due to a reduction in non-specific tissue binding.

Figure 9 cLogP correlates with Occ_{50}

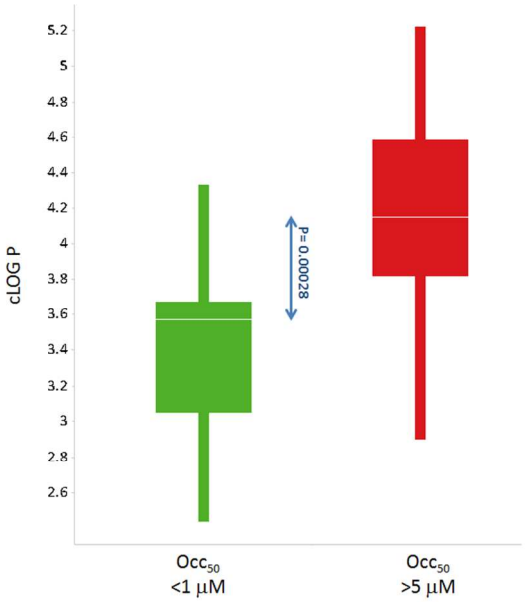

Figure 10 Calculated in vivo half-life correlates with duration of action

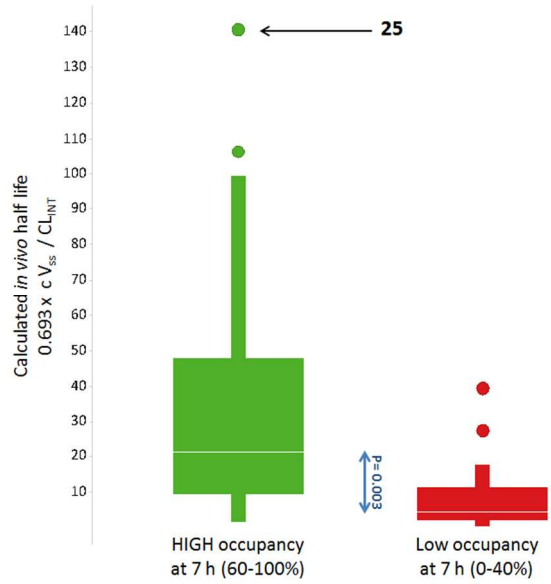

Within the set of molecules evaluated no direct correlations were seen between membrane affinity and occupancy. Furthermore a close link was observed between PK and PD across the compound set. This link suggests that, for these molecules at least, there is little role for variations in binding kinetics (K_{on}/K_{off}), in determining duration of action. Variations in binding kinetics would be expected to manifest themselves in a disconnect between PK and PD.

Using column methods it was possible to estimate a rat volume of distribution based on Rat HSA binding and CHI-IAM measurements[20] using this data and measurement of CL_{int} from rat liver microsomes it was possible to estimate an *in vivo* half-life for the compound set. This estimated number correlated well with duration of action ($p = 0.003$) (Figure 10) despite being essentially an estimate of systemic clearance, which did not take into account the effects of secondary metabolism, renal or biliary clearance. Interestingly the compounds with the best duration of action (e.g. **22** and **25**) were outliers in this analysis being the compounds with the highest predicted *in vivo* half-life. Purely by use of *in vitro* methods a prediction of duration of action for this compound class can be made. A possible interpretation of this empirical observation is that molecules with high predicted microsomal clearance are also metabolised in the lung tissue itself, leading to a shorter duration of action. Measurements of lung microsomal stability were not carried out for compounds within this series. Interestingly although systemic half-life was predicted to be very long for **25**, the molecule was primarily cleared by renal excretion of parent and had an *in vivo* half-life in rat of 14±3 h. This had the effect of reducing systemic exposure without compromising lung levels.

The comparison of the occupancy seen with **25** when dosed by the *it* and *iv* routes gives a clear indication of the enhanced therapeutic index obtained by the *it* delivery route, which is a consequence of depoting in the lung tissue as part of the absorption from the airways. The enhanced occupancy seen makes it clear that the depoted compound is also available at the site of action. For a given systemic exposure much more occupancy is achieved by the *it* route (Figure 11). Compound **25** showed high bioavailability after *it*

dosing (F= 90%) but a comparison of lung levels by the *it* and *iv* routes shows that the tissue distribution has been altered with a much higher lung: plasma ratio enabling enhanced lung efficacy to be achieved.

Figure 11 Comparison of Occupancy after *it* and *iv* dosing

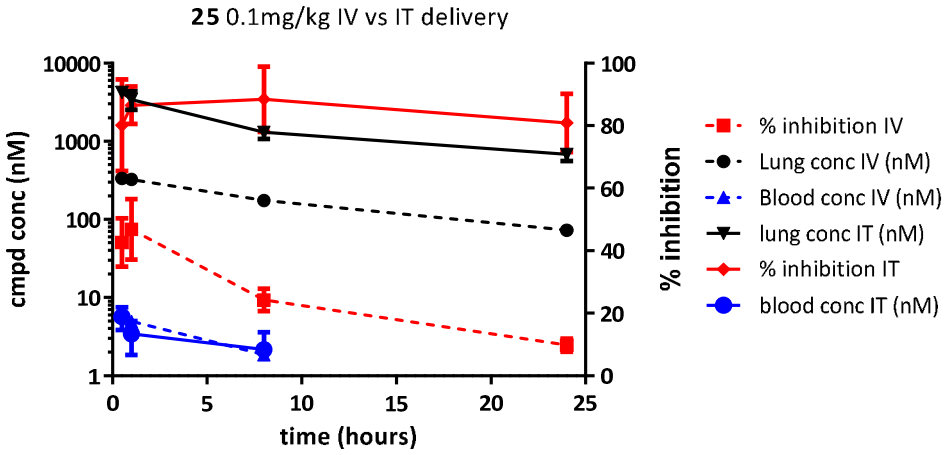

To confirm that the occupancy of the PDGFR kinase observed translated into inhibition of downstream signaling, the efficacy of **25** was assessed in a the monocrotaline (MCT) model of PAH. Pulmonary artery smooth muscle proliferation was measured in rats pretreated with monocrotaline for two weeks.[21] **25** was administered twice daily by the *it* route for seven days in a therapeutic mode (i.e. Pathology was allowed to develop before administration of the test compound). Oral administration of **1** was used as a positive control in the study, since it has shown efficacy in human clinical trials.

Compound **25** showed anti-remodeling efficacy against MCT induced Smooth muscle cell proliferation in the pulmonary vasculature (Figure 12). The minimum efficacious dose of **25** was 0.03 mg/kg (twice daily), which significantly reduces the percent of fully muscularized vessels to 14.3 (SEM = 1.6%) compared to 34.6 (SEM = 3.1%) in the MCT vehicle control group (A). Imatinib **1** significantly reduced the muscularization of small vessels at 100 mg/kg (A). However in a separate experiment, no efficacy was observed when administering **1** at 25 mg/kg, a dose which provides equivalent exposure to that achieved in patients receiving a 400 mg/day dose of **1** as part of the PAH Phase III clinical trial(B)[6]. This

comparative data suggest that clinical efficacy may be observed at drug exposures which were well below those required for efficacy in the monocrotaline model.

Figure 12 A) Efficacy of **25** (i.t.) in the rat Monocrotaline model of pulmonary hypertension in comparison to **1** (p.o), expressed as a percentage of fully muscularised small blood vessels within the lung upon histological evaluation B) Efficacy of a clinically relevant dose of **1** (p.o) in the rat Monocrotaline model of pulmonary hypertension expressed as a percentage of fully muscularised small blood vessels within the lung upon histological evaluation

A B

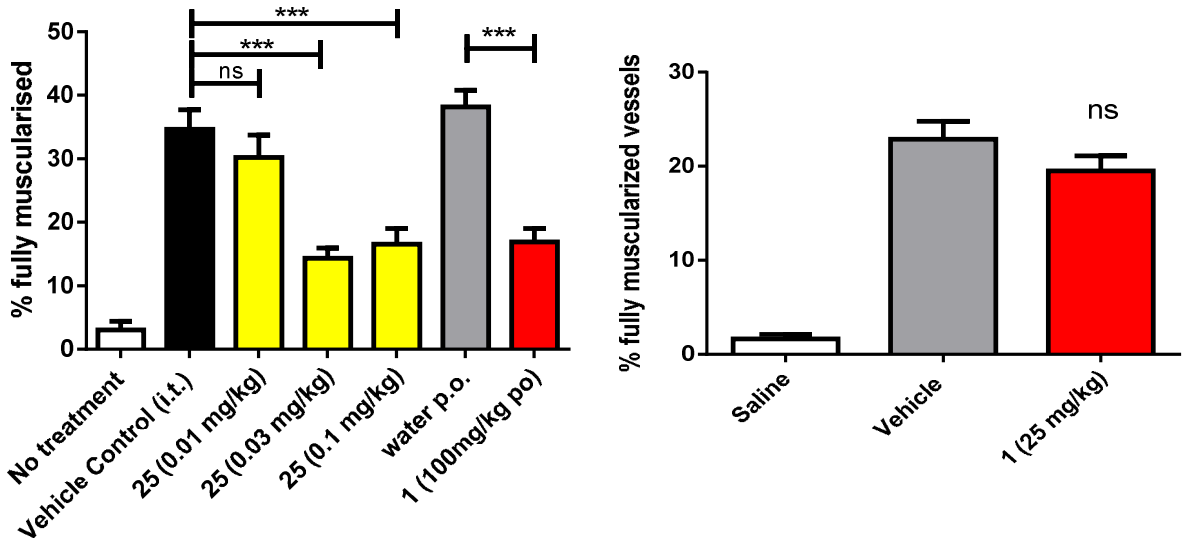

By using lower doses and *it* administration of compound the systemic burden in terms of blood levels is significantly reduced compared to oral administration of **1** (Table 5).

Table 5 Systemic exposure of test compound in the MCT model

Compound	Dose (mg/kg)	Blood Conc. (μM)
25	0.01	0.21 ± 0.081
25	0.03	0.75 ± 0.14
25	0.1	1.90 ± 0.31
1	100	305.5 ± 268.5

A Stable crystalline saccharin salt of **25** was identified as suitable for micronisation and Inhaled delivery as an aerosol. The compound was then administered to rats at 0.79 mg/kg of as a micronized dry powder[22], over 1 hour and showed occupancy consistent with that seen after *it* dosing given the expected delivery efficiency of 10% (Figure 13).

Figure 13 Occupancy seen after inhaled dosing of **25** saccharinate salt

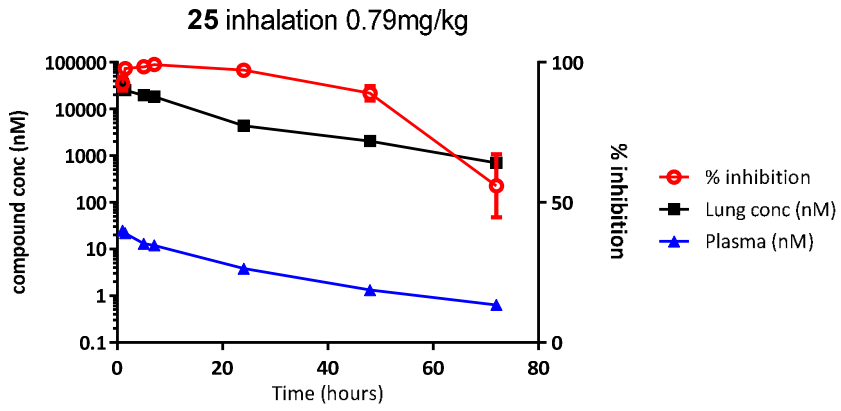

Compound **25** showed good selectivity in a receptor panel of 85 assays at Ricerca with no significant activity at 10 μM, confirming an excellent selectivity observed in an in house screening panel of 45 GPCRs and Ion channels. A selectivity screen of 451 kinases at DiscoverX revealed 31 interactions a selectivity score S(35) = 0.08. These interactions were as expected in the PDGFR/KIT and SRC families of receptor tyrosine kinases and pleasingly showed a very similar pattern of selectivity to that seen with **1**.[23] (Figure 14).

Figure 14 Kinome tree plot for **25**

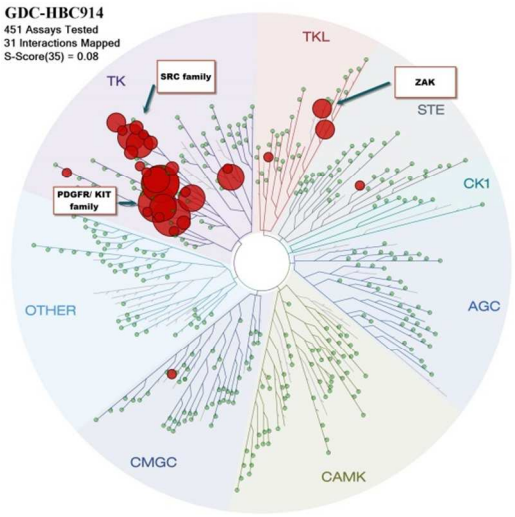

CONCLUSION

We have established that efficacy in the whole lung can be achieved, whilst maintaining an enhanced therapeutic index over systemic delivery. Within our series of soluble, basic molecules the desired properties for duration of action have been highlighted. Low permeability has been shown to be important for this series of molecules, and the beneficial effect of high pKa has also been demonstrated. The effect of a highly basic group has been noted before in inhaled drug design[7] as has the presence of a second less basic centre[7] and this study reconfirms this finding starting from an unbiased analysis of *in vitro*: *in vivo* correlations. The size of this effect has been quantified for this series of molecules. The effect of non-specific binding to tissues is a clear factor, and the correlation between cLogP and Occ_{50} is perhaps unsurprising given that basic molecules already have an affinity for tissues. Combining basicity with high lipophilicity is likely to lead to extensive non-specific binding to tissue and to limit the percentage of free drug available to achieve occupancy. The wider applicability of these findings to inhaled drug design in general would be supported by direct measurement of PK-PD at other targets and in more diverse chemical space. Corroboration of these findings from the literature does exist but the importance of directly measuring pharmacodynamics as well as pharmacokinetics when assessing therapeutic index and

duration of action has been emphasized by problems encountered within other inhaled drug discovery projects.[7]

Indeed within this series, high drug levels in the lung have been observed for multiple molecules without correspondingly high target occupancy (e.g. **16**), by measuring the PD in the same animal at the same time point, it can be established that drug present is binding to the target.

By using solutions in our *it* dosing experiments, we have eliminated the effects of solid form and dissolution rate from our measurements of duration of action, and have thereby assessed the intrinsic ability of the molecules to depot in lung tissue as part of the first pass absorption. By using a soluble molecule when dosing *it*, we essentially looked at the worst case scenario for duration of action. The inhaled dosing of a solid form will generally allow for increased duration based on dissolution rate factors. The Inhalation PK and PD of the lead molecule **25** as a saccharin salt validate our assumption that the intrinsic depoting properties and duration of action would not be adversely affected by dosing route and solid form factors.

This approach has allowed us to identify **25**, a potent PDGFR antagonist (10 fold more potent than **1** in cell based proliferation assays) with a selectivity profile similar to that of **1**, which shows excellent duration of action after a single low dose in our PK/PD model.

Comparison of the same dose delivered by the *it* route and by the *iv* route demonstrates clearly the significant perturbation of the drug distribution to lung obtained by changing dosing route. This is coupled with a clear demonstration that the extra drug levels in the lung lead to enhanced occupancy and duration of action (80 % at 24h after *it* dose vs 10 % at 24h after *iv* dose). This finding predicts a lower absolute dose requirement in the clinic since a far greater proportion of the dose delivered is reaching the target tissue and is delivering occupancy.

Importantly we have shown that the occupancy obtained translates into efficacy in the MCT model of PAH in rat and that the Minimum effective dose, 0.03 mg/kg (*it* /bid.) is significantly reduced compared to the dose of **1** which is effective in the model 100 mg/kg (*p.o.* /q.d.).

The IMPRESS trial with oral Imatinib successfully demonstrated efficacy in PAH but was hampered by side effect driven patient withdrawals. As an inhaled compound **25** has the potential to deliver the efficacy in patients with much lower systemic exposure to drug and to allow greater inhibition of the target in the lung without similar tolerability issues. Further characterization of **25** will be reported in due course.

EXPERIMENTAL

General Conditions:

Compounds were confirmed to be of ≥95% purity or greater by LCMS (methods described below) Mass spectra were run on LCMS systems using electrospray ionization, using Waters Acquity UHPLC with SQD Mass Spectrometer. $[M+H]^+$ refers to mono-isotopic molecular weights. Purity of tested compounds was determined by LCMS 5 minute run (Method 1: ACQUITY UHPLC BEH C18, 130Å, 1.7 µm, 2.1 mm X 50 mm, Temp 50°C; flow rate 1.0 mL/min, Eluents A H_2O containing 5 mM ammonium hydroxide; B Acetonitrile containing 5 mM ammonium hydroxide; Gradient 0.06 min 2% B, 2%-98% B in 4.40 min, 0.35 min 98% B). Intermediates were characterized using a 2 minute LCMS run (Method 2: Column Waters BEH C18 50x2.1 mm, 1.7 µm, Temp 50°C; flow rate 0.8 mL/min, Eluents A H_2O; B MeOH containing 0.1 % TFA; Gradient 0.2 min 5% B, 5%-95% B in 1.30 min, 0.25 min 95% B). Structural confirmation was by ^1H NMR and ^{13}C NMR in conjunction with High Resolution Mass Spectrometry (HRMS). NMR spectra were run on Bruker AVANCE 400 NMR spectrometers using ICON-NMR. Spectra were measured at 298K and were referenced using the solvent peak. HRMS was measured on an Acquity G2 Xevo QTof machine. Melting points were determined by differential scanning calorimetry.

N-(2-fluoro-5-((2-(4-methylpiperazin-1-yl)benzyl)carbamoyl)phenyl)imidazo[1, 2-a]pyridine-3-carboxamide 2; Methyl 3-amino-4-fluorobenzote (350 mg, 2 mmol) and imidazo[1, 2-a]pyridine-3-carbonyl chloride (411 mg, 2.2 mmol) were combined in pyridine (7.5 mL) and stirred for 16 h. The reaction mixture was diluted with chloroform and washed with water (x 2), and then the organic layer was washed with 1M HCl, sat. aq. sodium bicarbonate, and then brine, the organic layer was then dried ($MgSO_4$) and evaporated. The residue was triturated with ethyl acetate and **5b** (448 mg, 1.3 mmol, 65% yield) was obtained as a white solid. ^{1}H NMR, (D6-DMSO, 400 mHz) δ 13.14 (1H, br s), 10.31 (1H, s), 9.48 (1H, d), 8.64 (1H, s), 8.28 (1H, m), 7.87 (1H, m), 7.80 (1H, d), 7.57 (1H, m), 7.46 (1H, m), 7.23 (1H, m).

5b (100 mg, 0.319 mmol), (2-(4-methylpiperazin-1-yl)phenyl)methanamine (197 mg, 0.958 mmol), and 1,5,7-Triazabicyclo[4.4.0]dec-5-ene (TBD) (133 mg, 0.958 mmol) were combined in THF (3 mL), the mixture was then heated to 70°C for 16h. The mixture was evaporated and the residue then purified by column chromatography on silica eluting with 0-15% Methanol in DCM. The desired fractions were collected , evaporated and precipitated with ethyl acetate to give as a white solid **2** (20mg, 0.319 mmol, 24% yield). mp = 71.2^{o}C; LCMS Method 1; Rt. 1.85 min; [MH]+ m/z 487.2; purity 95% ^{1}H NMR, (D6-DMSO, 400 mHz) δ 10.30 (1H, s), 9.47 (1H, d), 9.01 (1H, t), 8.62 (1H, s), 8.21 (1H, m), 7.86 (1H, m), 7.80 (1H, d), 7.57 (1H, m), 7.50 (2H, m), 7.18 (5H, m), 4.61 (2H, d), 3.18 (3H, s), 3.01 (8H, m). ^{13}C NMR($CDCl_3$, 100 MHz) 166.0, 158.4, 155.4, 153.0, 150.4, 148.7, 137.1, 132.9, 131.4, 130.1, 129.1, 128.0, 127.9, 126.3, 125.5, 124.2, 121.4, 118.0, 117.7, 115.9, 114.6, 55.0, 55.0, 50.9, 50.9, 44.7, 41.2; HRMS (ESI): m/z (MH^+) 487.2225. Calcd. 486.2257.

N-(5-(benzylcarbamoyl)-2-methylphenyl) pyrazolo [1, 5-a] pyridine-3-carboxamide 3; 3-Amino-4-methylbenzoic acid **4a** (423 mg, 2.77 mmol) was dissolved in DCM, Triethylamine (385 µl, 2.77 mmol) and pyrazolo [1, 5-a] pyridine-3-carbonyl chloride (500 mg, 2.77 mmol) were added. The reaction mixture was stirred for 30 min at RT then was poured into a separation funnel containing water. The organic layer was collected and the aqueous layer was extracted with DCM (x3). The combined organic

layers were dried ($MgSO_4$), filtered and evaporated to dryness. The product was recrystallized in MeOH and after filtration 4-methyl-3-(pyrazolo [1, 5-a] pyridine-3-carboxamido) benzoic acid **5a** was obtained (716 mg, 2.4 mmol 87% yield) of pure compound. LCMS Method 1; Rt. 0.54 min; [MH]+ m/z 296.1; purity 99% ^{1}H NMR, (D6-DMSO, 400 mHz) δ 12.82 (1H, s), 9.69 (1H, s), 8.84 (1H, d), 8.78 (1H, s), 8.22 (1H, d), 7.99 (1H, d), 7.72 (1H, dd), 7.53 (1H, dd), 7.40 (1H, d), 7.21 (1H, dd), 2.32 (3H, s).

5a (42 mg, 0.14 mmol) was dissolved in DMF (1.0 mL) and treated with HATU (58 mg, 0.152 mmol) and Triethylamine (59 μL 0.42 mmol). To this solution was added benzyl amine (18 mg, 0.17 mmol). The reaction mixture was stirred at room temperature overnight and then diluted with water. The aqueous was washed with 0.5M LiCl, 0.5M citric acid and then brine. The organic layer was dried ($MgSO_4$) and concentrated *in vacuo* then purified by chromatography on silica eluting with 0-100% ethyl acetate in heptane. **3** (22mg, 6 mmol, 38% yield) was obtained as a white solid. mp = 183^{o}C ; LCMS Method 1; Rt. 1.83 min; [MH]+ m/z 385.2; purity 99% ^{1}H NMR, (D6-DMSO, 400 mHz) δ 9.74 (1H, s), 9.03 (1H, t), 8.82 (1H, d), 8.76 (1H, s), 8.22 (1H, d), 7.93 (1H, s), 7.87 (1H, m), 7.74 (1H, d), 7.52 (1H, m), 7.39 (1H, d), 7.31 (3H, m), 7.23(1H, m), 7.14 (1H, t), 4.46 (2H, d), 2.31 (3H, s). ^{13}C NMR (D6-DMSO, 100 MHz) 164.6, 160.1, 140.7, 139.2, 138.7, 131.2, 129.2, 128.5, 127.1, 126.15, 126.12, 125.6, 124.6, 123.4, 117.6, 114.3, 112.9, 105.1, 41.4, 17.0; HRMS (ESI): m/z (MH^+) 385.1653. Calcd. 385.1664.

methyl 5-amino-6-methylnicotinate 4c

To a suspension of 6-methyl-5-nitro-2-oxo-1, 2-dihydropyridine-3-carboxylic acid **8** (12.5 g, 63.1 mmol) in chlorobenzene (210 mL) was added DMF (2.4 mL, 31.5 mmol) followed by $POCl_3$ (23.5 mL, 252 mmol). The mixture was heated at 133 °C for 1 hr. After cooling to RT, the mixture was concentrated *in vacuo*. The residue was cooled in an ice bath, treated with MeOH (200 mL, 4944 mmol) and stirred at RT for 16h. The mixture was concentrated *in vacuo* and the residue was partitioned between water (300 mL) and EtOAc (300 mL). The organics were dried ($MgSO_4$) and concentrated *in vacuo* to afford **9** as a red crystalline solid (11.8g, 41 mmol, 80% yield); LCMS Method 2; Rt 1.10 min; $[MH]^+$ m/z 230.9.

6e was prepared from **5e** in a similar manner to **6c**

LCMS: Method 2; Rt 0.69 min; $[MH]^+$ m/z 377.5. ^{1}H NMR (400 MHz, DMSO) δ 13.35 (1H, s), 9.89 (1H, s), 9.18 (1H, s), 8.83 (1H, s), 8.78 (1H, s), 8.34 (2H, d), 8.22 (1H, d), 8.07 (1H, s), 7.82 (1H, d), 3.89 (3H, s), 2.56 (3H, s).

5e was prepared from **4c** in a similar manner to **5a**

LCMS: Method 2; Rt 0.91 min; $[MH]^+$ m/z 391.4. ^{1}H NMR (400 MHz, DMSO) δ 10.01 (1H, s), 9.32 (1H, s), 8.89 (1H, d), 8.83 (1H, s), 8.38 (1H, d), 8.18 (1H, d), 7.71 (1H, d), 3.93 (3H, s), 2.61 (3H, s).

9 (6.9 g, 29.9 mmol) was added to a suspension of ammonium formate (18.87 g, 299 mmol) and 10% Pd/C (0.522 g, 0.491 mmol) in MeOH (330 mL) and the mixture was heated at reflux for 3 h. After cooling to RT, the mixture was filtered through Celite and washed through with MeOH. The solvent was removed *in vacuo* and the crude product was triturated with EtOAc to give an orange solid. Purification by chromatography on silica eluting with 0-100% EtOAc in iso-hexane afforded **4c** (5.9g, 35.5 mmol, 76% yield). LCMS: Method 2; Rt 0.25 min; $[MH]^+$ m/z 166.8. ^{1}H NMR (400 MHz, $CDCl_3$) δ 8.58 (1H, s), 7.52 (1H, s), 3.94 (3H, s), 3.76 (2H, brs), 2.49 (3H, s).

(5, 5-Dimethyltetrahydrofuran-2-yl)methanamine 11;

10 (36 g, 186 mmol) in DMF (300 mL) was treated with solid sodium azide (12.7 g, 196 mmol) and heated at 90°C for 4 h. The mixture was allowed to cool to RT and partitioned between water (1.5 L) and ether (2 x 500 mL). The ether layer was separated and washed with 0.5M LiCl (500 mL), dried ($MgSO_4$), filtered and evaporated to afford 5-(Azidomethyl)-2, 2-dimethyltetrahydrofuran (22 g, 142 mmol). The product was dissolved in THF (500 mL), treated with Triphenylphosphine (39.0 g, 149 mmol) and stirred for 5 min. Water (50.0 mL) was added and the reaction mixture was heated at 80°C for 4 h. The mixture was passed through Isolute SCX-2 resin (200g, 0.67 mmol /g) eluting with MeOH(500 mL), DMSO (100 mL), 20% MeOH:DCM (500 mL) and MeOH (500 mL) followed by elution of the product with 7M ammonia in MeOH (500 mL). The ammonia layer was evaporated to dryness to afford the **11** (7.95g, 61 mmol, 43% yield) LCMS: Method 2; Rt 063 min; $[MH]^+$ m/z 243.0. ^{1}H NMR (400 MHz, $CDCl_3$) δ 4.03-

3.95 (1H, m), 2.80 (1H, dd), 2.68 (1H, dd), 2.06-1.94 (1H, m), 1.79-1.63 (3H, m), 1.24 (3H, s), 1.26 (3H, s).

N-(2-fluoro-5-((2-(4-methylpiperazin-1-yl)benzyl)carbamoyl)phenyl)-7-(pyridin-3-yl)imidazo[1, 2-a]pyridine-3-carboxamide 12; 7-bromoimidazo[1, 2-a]pyridine-3-carboxylic acid (1.8 g, 7.47 mmol) and thionyl chloride (10 mL, 137 mmol) were heated at reflux for 1.5 h. The reaction mixture was concentrated in *vacuo* and azeotroped with toluene. Methyl 3-amino-4-fluorobenzoate (1.263 g, 7.47 mmol) was added followed by pyridine and the mixture was stirred at room temperature overnight. The reaction mixture was diluted with EtOAc and washed with H_2O. The resulting solid was collected by filtration. The filtrate was dried ($MgSO_4$) and concentrated *in vacuo* and triturated with ether to afford cream solid. The solids were combined and dried at 45^oC to afford **5c**; LCMS: Method 2; Rt 0.97 min; [MH]+ m/z 392; ^{1}H NMR (400MHz, DMSO-d6) δ 10.3 (1H, s), 9.4 (1H, d), 8.6 (1H, s), 8.3 (1H, m), 8.2 (1H, s), 7.9 (1H, m), 7.5 (1H, t), 7.4 (1H, d), 3.9 (3H, s).

5c (1.08 g, 2.75 mmol), TBD (0.383 g, 2.75 mmol) and (2-(4-methylpiperazin-1-yl) phenyl) methanamine (0.565 g, 2.75 mmol) in toluene (35 mL) were heated to 80°C overnight. Toluene was removed *in vacuo* and the resulting solid was partitioned between aqueous sodium bicarbonate solution and EtOAc. The organic portion was washed with sodium bicarbonate solution (2 x 50 mL) and concentrated in vacuo. The resulting oil was purified by chromatography on silica eluting with 0-10% MeOH in DCM. The fractions were combined and the solvent removed *in vacuo*. The resulting solid was recrystallized from EtOAc (50 mL) to afford **7c** (457 mg, 0.78 mmol, 28% yield).; LCMS: Method 2; Rt 0.85 min; $[MH]^+$ m/z 567.4 ^{1}H NMR (400MHz, d6-DMSO) δ 10.3 (1H, s), 9.4 (1H, d), 8.9 (1H, t), 8.6 (1H, s), 8.2 (1H, d), 8.1 (1H, s), 7.8 (1H, m), 7.4 (1H, d), 7.35 (1H, d), 7.2 (2H, m), 7.1 (1H, d), 7.0 (1H, t), 4.6 (1H, d), 2.9 (4H, m), 2.4 (3H, t), 2.2 (3H, s).

Under nitrogen, **7c** (120 mg, 0.212 mmol), pyridine-3-ylboronic acid (33.8 mg, 0.212 mmol), triethylamine (0.030 mL, 0.212 mmol), cesium carbonate (69.1 mg, 0.212 mmol) and $PdCl_2$(dppf).CH_2Cl_2 adduct (17.3 mg, 0.021 mmol) in DMF (3 mL) were heated at 85 ℃ overnight. The reaction mixture was

diluted with EtOAc and water. The organic phase, which was washed with sat. aq. sodium bicarbonate and brine, then dried ($MgSO_4$) and concentrated *in vacuo*. The crude residue was purified by chromatography on silica eluting with 0-20% MeOH/DCM. To yield **12** (12 mg 0.21 mmol, 10% yield); mp = 153.5°C; LCMS Method 1; Rt. 1.89 min; $[MH]^+$ m/z 564.2; purity >99% ^{1}H NMR (400MHz, CD_3OD) δ 9.7 (1H, d), 9.1 (1H, d), 8.7 (1H, m), 8.6 (1H, s), 8.4 (1H, m), 8.3 (1H, m), 8.2 (1H, s), 8.1 (1H, s), 7.8 (1H, m), 7.7-7.5 (2H, m), 7.4-7.1 (5H, m), 4.3 (2H, s), 3.1 (4H, m), 2.8 (4H, s broad), 2.5 (3H, t). ^{13}C NMR(D6-DMSO, 100 MHz) 164.5, 158.0, 155.6, 150.0, 149.0, 147.2, 138.7, 135.3, 133.7, 132.8, 132.1, 130.2, 127.2, 127.0, 126.9, 126.0, 125.4, 124.4, 123.4, 122.8, 118.7, 116.9, 115.4, 115.2, 113.7, 112.6, 54.5, 54.5, 51.2, 51.2, 45.0, 37.7; HRMS (ESI): m/z (MH^+) 564.2512. Calcd. 564.2523.

N-(2-fluoro-5-((2-(4-methylpiperazin-1-yl)benzyl)carbamoyl)phenyl)-7-(1-methyl-1H-pyrazol-5-yl)imidazo[1, 2-a]pyridine-3-carboxamide 13; was prepared from **7c** in a similar manner to **8** LC-MS: mp 244.4°C; LCMS Method 1; Rt. 1.89 min; $[MH]^+$ m/z 567.3; purity 98.8% ^{1}H NMR (400MHz, MeOD) δ 9.6 (1H, s), 8.6 (1H, s), 8.4 (1H, m), 7.9 (1H, s), 7.8 (1H, m), 7.6 (1H, s), 7.45-7.3 (5H, m), 7.2 (1H, m), 6.7 (1H, s), 4.75 (2H, s), 4.1 (3H, s), 3.4 (4H, s broad), 3.2 (4H, s broad), 2.95 (3H, s). ^{13}C NMR(D6-DMSO, 100 MHz) 164.5, 158.0, 155.6, 150.0, 146.5, 139.4, 138.6, 137.5, 132.8, 130.2, 128.3, 127.0, 126.9, 126.1, 124.4, 124.3, 122.7, 118.7, 117.0, 115.4, 115.2, 115.0, 114.0, 106.4, 54.6, 54.6, 51.3, 51.3, 45.2, 37.7, 37.5; HRMS (ESI): m/z (MH^+) 567.2618. Calcd. 567.2632.

N-(2-fluoro-5-((2-(4-methylpiperazin-1-yl)benzyl)carbamoyl)phenyl)-7-(1-methyl-1H-pyrazol-4-yl)imidazo[1, 2-a]pyridine-3-carboxamide 14; was prepared from **7c** in a similar manner to **8** LC-MS: mp 189.5°C; LCMS Method 1; Rt. 1.85 min; $[MH]^+$ m/z 567.2; purity 97.9% ^{1}H NMR (400MHz, D6-DMSO) δ 10.21(1H, s), 9.32 (1H, d), 8.95 (1H, s), 8.57 (1H, s), 8.42 (1H, s), 8.22 (1H, d), 8.13 (1H, s), 7.98 (1H, s), 7.83-7.88 (1H, m), 7.42-7.48 (2H, m), 7.18-7.26 (2H, m), 7.15 (1H, d), 4.58 (2H, d), 3.89 (3H, s), 2.98 (4H, s broad), 2.51 (4H, s broad), 2.26 (3H, s). ^{13}C NMR(D6-DMSO, 100 MHz) 164.4, 158.2, 156.7, 155.6, 148.6, 141.7, 137.6, 137.2, 133.3, 130.3, 130.2, 128.5, 127.5, 127.1, 126.2, 126.0,

123.8, 119.2, 117.7, 117.4, 115.5, 115.3, 115.0, 105.1, 53.4, 53.4 48.4, 48.4 41.5, 38.4, 37.7; HRMS (ESI): m/z (MH^+) 567.2637. Calcd. 567.2632.

N-(2-fluoro-5-((2-(4-methylpiperazin-1-yl)benzyl)carbamoyl)phenyl)-7-(1H-pyrazol-3-yl)imidazo[1, 2-a]pyridine-3-carboxamide 15; was prepared from **25c** in a similar manner to **8**. mp 123.8^{o}C; LCMS Method 1; Rt. 1.80 min; $[MH]^+$ m/z 553.3; purity >99% ^{1}H NMR (400MHz, D6-DMSO) δ 13.17 (1H, s), 10.26(1H, s), 9.43 (1H, d), 8.98 (1H, t), 8.61 (1H, s), 8.22 (1H, d), 8.15 (1H, s), 7.98 (1H, s), 7.84-7.91 (1H, m), 7.71 (1H, d), 7.45 (1H, t), 7.28-7.22 (2H, m), 7.18-7.02 (3H, m), 4.58 (2H, d), 3.89 (3H, s), 2.84-2.92 (8H, s broad), 2.51 (4H, s broad), 2.25 (3H, s). ^{13}C NMR(D6-DMSO, 100 MHz) 164.5, 158.0, 155.6, 150.1, 147.4, 147.3, 138.5, 132.8, 132.5, 130.2, 129.9, 127.0, 126.9, 126.0, 124.5, 124.4, 122.8, 118.7, 116.9, 115.4, 115.1, 111.5, 111.1, 102.4, 54.5, 54.5, 51.3, 51.3, 45.2, 37.7; HRMS (ESI): m/z (MH^+) 553.2470. Calcd. 553.2476.

N-(5-((3, 4-difluorobenzyl)carbamoyl)-2-fluorophenyl)-7-(1-methyl-1H-pyrazol-5-yl)imidazo[1, 2-a]pyridine-3-carboxamide 16; was prepared from **7c** in a similar manner to **8**. mp 222.7^{o}C; LCMS Method 1; Rt. 2.00 min; $[MH]^+$ m/z 505.2; purity >99% ^{1}H NMR (400 MHz, DMSO) δ 10.35 (1H, s), 9.50 (1H, d), 9.17 (1H, t), 8.68 (1H, s), 8.19 (1H, d), 8.00 (1H, s), 7.75 (1H, m), 7.56 (1H, s), 7.42-7.50 (3H, m), 7.18 (1H, m), 4.48 (2H, d), 4.01 (3H, s). ^{13}C NMR(D6-DMSO, 100 MHz) 164.4, 158.0, 155.6, 146.6, 139.6, 138.6, 137.5, 129.9, 128.3, 127.0, 126.0, 125.5, 124.4, 123.4, 117.0, 116.8, 116.6, 115.7, 115.5, 115.4, 115.3, 115.1, 114.0, 106.4, 41.3, 37.5; HRMS (ESI): m/z (MH^+) 505.1598. Calcd. 505.1600.

N-(5-(((5, 5-dimethyltetrahydrofuran-2-yl)methyl)carbamoyl)-2-fluorophenyl)-7-(1-methyl-1H-pyrazol-5-yl)imidazo[1, 2-a]pyridine-3-carboxamide 17; was prepared from **7c** in a similar manner to **8** LCMS Method 1; Rt. 1.83 min; $[MH]^+$ m/z 491.2; purity 95.0% ^{1}H NMR (400 MHz, DMSO) δ 10.54 (1H, s), 9.53 (1H, d), 8.84 (1H, s), 8.62 (1H, t), 8.17 (1H, dd), 8.09 (1H, s), 7.86-7.81 (1H, m), 7.62-7.42 (3H, m), 6.73 (1H, s), 4.10-4.05 (1H, m), 4.03 (3H, s), 3.37-3.25 (2H, m), 2.06-1.92 (1H, m), 1.78-1.65 (3H, m), 1.22 (3H, s), 1.15 (3H, s) ^{13}C NMR(D6-DMSO, 100 MHz) 165.3, 158.6, 156.6, 140.3, 138.7, 131.5, 131.4, 128.5, 127.2, 125.2, 125.0, 124.7, 118.4, 116.5, 116.2, 116.0, 114.9, 107.9, 81.0, 77.1, 44.8, 38.7, 38.1, 29.7, 29.6. 28.4; HRMS (ESI): m/z (MH^+) 491.2228. Calcd. 491.2206.

N-(5-((2-(2, 6-cis-dimethylpiperidin-1-yl)ethyl)carbamoyl)-2-fluorophenyl)-7-(1-methyl-1H-pyrazol-5-yl)imidazo[1, 2-a]pyridine-3-carboxamide 18; was prepared from **7c** in a similar manner to **8**; m.p. 141.1°C; LCMS: Method 1; Rt. 1.42 min; $[MH]^+$ m/z 518.3; purity >99% ^{1}H NMR (400MHz, DMSO) δ 10.71 (1H, s), 10.01 (1H, t), 9.72 (1H, d), 9.33 (1H, s), 9.05 (1H, m), 8.90 (1H, s), 8.85 (1H, d), 8.70 (1H, m), 8.47 (1H, s), 8.23 (1H, m), 7.89 (3H, m), 7.51 (1H, m), 3.55 (2H, m), 3.50-3.33 (2H, m), 1.83 (1H, m), 1.70 (2H, m), 1.50 (2H, m), 1.40 and 1.30 (6H, 2 x d). ^{13}C NMR(D6-DMSO, 100 MHz) 164.7, 158.6, 158.3, 147.2, 140.2, 139.2, 138.1, 130.9, 128.9, 127.6, 126.4, 125.9, 124.9, 117.7, 115.8, 114.6, 107.0, 55.9, 55.9, 47.5, 38.1, 37.0, 34..4, 34.4, 24.2. 21.3, 21.3; HRMS (ESI): m/z (MH^+) 518.2674. Calcd. 518.2680.

N-(5-((2-(tert-butyl(methyl)amino)ethyl)carbamoyl)-2-fluorophenyl)-7-(1-methyl-1H-pyrazol-5-yl)imidazo[1, 2-a]pyridine-3-carboxamide. Hydrochloride salt 19;

5c (1.5 g, 3.82 mmol), 1-methyl-5-(4, 4, 5, 5-tetramethyl-1, 3, 2-dioxaborolan-2-yl)-1H-pyrazole (0.836 g, 4.02 mmol), Cs_2CO_3 (4.98 g, 15.30 mmol) and $PdCl_2$(dppf).DCM adduct (0.156 g, 0.191 mmol) were combined in DME (12 mL) and Water (5 mL). The mixture was degassed thoroughly refilling with nitrogen (x3). The mixture was stirred at 100 C for 6h in the microwave. The reaction mixture was diluted with EtOAc and water and the resulting product which precipitated out was collected by filtration. The organic phase, was washed with sat. $NaHCO_3$, brine, dried ($MgSO_4$) and concentrated *in vacuo*. The crude residue was combined with the precipitated product and purified by chromatography on silica eluting with 0-10% MeOH/DCM. **6a** (1g, 2.54 mmol, 66% yield) was obtained.

6a (650 mg, 1.6 mmol) in Methanol (40mL) and DCM (10 mL) was treated with sodium hydroxide (132.1 mg, 3.2 mmol) and, warmed to 80°C overnight. The reaction was cooled to r.t. and 1M HCl in methanol was added in excess. The cold mixture was filtered and then the solvent was removed *in vacuo* to give **6b** as the hydrochloride salt (600 mg, 1.58 mmol, 96% yield).

6b (120 mg, 0.289 mmol) and 2-(tert-butyl (methyl)amino)ethanaminium 2, 2, 2-trifluoroacetate (71 mg 0.289 mmol) were combined in DMF (5 mL) and treated with Disopropylethylamine (0.353 mL, 2.020

mmol) and then HATU (115 mg, 0.303 mmol) at 25 °C for 16 hr. The residue was partitioned between ethyl acetate and water and then the aqueous was back extracted with ethyl acetate. The combined organics were washed with 0.5M LiCl. and then brine, the combined organic layers were dried ($MgSO_4$), filtered and evaporated to dryness (90mg). The residue was purified by column chromatography eluting with 0-10% MeOH (containing 2M ammonia) in DCM. The desired fractions were evaporated to dryness then were suspended in ethanol and treated with 4M HCl in dioxane before evaporating to dryness. azeotroping with ethyl acetate and ethanol to give **19** (35 mg, 0.066 mmol, 23 % yield). LCMS Method 1; Rt. 1.78 min; $[MH]^+$ m/z 492.3; purity 95% ^{1}H NMR (400 mHz, D6-DMSO) δ 10.40 (1H, s), 9.50 (1H, d), 9.35 (1H, m), 8.90 (1H, m), 8.73 (1H, m), 8.25 (1H, d), 8.05 (1H, s), 7.86 (1H, m), 7.57 (1H, s), 7.52-7.40 (2H, m), 6.7 (1H, s), 4.05 (3H, s), 3.55 (2H, m), 3.05 (2H, m), 2.80 (3H, s), 1.35 (9H, s). ^{13}C NMR(D6-DMSO, 100 MHz) 163.1, 157.0, 156.2, 154.5, 137.8, 136.4, 128.3, 126.3, 125.0, 122.9, 114.3, 113.9, 112.0, 105.6, 61.3, 48.5, 36.3, 33.2, 32.8, 21.7. 21.7, 21.7; HRMS (ESI): m/z (MH^+) 492.2536. Calcd. 492.2523.

N-(5-((2-(tert-butyl(ethyl)amino)ethyl)carbamoyl)-2-fluorophenyl)-7-(1-methyl-1H-pyrazol-5-yl)imidazo[1, 2-a]pyridine-3-carboxamide 20; was prepared from **6b** in a similar manner to **19**. LCMS Method 1; Rt. 2.14 min; $[MH]^+$ m/z 506.3; purity 95%. ^{1}H NMR (400 mHz, D6-DMSO) δ 1.37 (12H, m), 10.50 (1H, s). 9.60 (1H, d), 9.40 (1H, m), 9.10 (1H, m), 8.80 (1H, m), 8.25 (1H, d), 8.07 (1H, s), 7.90 (1H, m), 7.57 (1H, s), 7.51(2H, m), 6.73 (1H, s), 4.05 (3H, s), 3.75 (2H, m), 3.47 (2H, m), 3.15 (2H, m). ^{13}C NMR(D6-DMSO, 100 MHz) 165.5, 159.3, 158.5, 156.9, 140.1, 138.7, 131.6, 130.6, 128.7, 127.2, 126.5, 125.4, 125.3, 116.7, 116.5, 116.4, 114.3, 108.0, 65.4, 49.2, 46.3, 38.7, 37.4, 24.5, 24.5, 24.5, 11.3; HRMS (ESI): m/z (MH^+) 506.2675. Calcd. 506.2680.

N-(5-((2-(2, 2-dimethylpyrrolidin-1-yl)ethyl)carbamoyl)-2-fluorophenyl)-7-(1-methyl-1H-pyrazol-5-yl)imidazo[1, 2-a]pyridine-3-carboxamide 21; was prepared from **6b** in a similar manner to **19**. LCMS Method 1; Rt. 2.00 min; $[MH]^+$ m/z 504.3; purity 95.1% ^{1}H NMR (400 mHz, D6-DMSO) δ. 10.50 (1H, s), 9.90 (1H, m), 9.40 (1H, d), 8.95 (1H, m), 8.78 (1H, m), 8.24 (1H, d), 8.04 (1H, s), 7.90 (1H, m), 7.57

(1H, s), 7.49 (2H, m), 6.71 (1H, s), 4.05 (3H, s), 3.70 (2H, m), 3.57 (1H, m), 3.25 (1H, m), 3.15 (1H, m), 1.95 (4H, m), 1.20 (6H, m), 3.35 (1H, m). ^{13}C NMR(D6-DMSO, 100 MHz) 165.5, 159.3, 158.7, 156.8, 140.3, 138.7, 130.7, 128.5, 127.3, 126.7, 125.4, 125.2, 118.4, 116.6, 116.4, 116.0, 114.9, 107.8, 59.3, 50.8, 47.7, 38.7, 37.2, 36.0, 22.9, 19.9, 19.8; HRMS (ESI): m/z (MH^+) 504.2522. Calcd. 504.2523.

N-(5-((2-(2, 2-dimethylpyrrolidin-1-yl)ethyl)carbamoyl)-2-fluorophenyl)-7-(1-methyl-1H-pyrazol-4-yl)imidazo[1, 2-a]pyridine-3-carboxamide 22.

A mixture comprising **5c** (5.4 g, 13.8 mmol), 1-methyl-1H-pyrazol-4-ylboronic acid (1.9 g, 15.2 mmol), Pd(dppf)Cl_2.DCM (1.1 g, 1.379 mmol) and cesium carbonate (13.5 g, 41.4 mmol) in DME (100 mL) and water (10mL) was heated at 100°C for 4 h. Sodium carbonate (8.9g, 84 mmol) was added and the reaction was heated at 100°C overnight. The reaction mixture was cooled to 50°C and filtered through glass fiber filter paper. The filtrate was acidified to pH 3 and allowed to cool to room temperature. A brown precipitate formed which was collected by vacuum filtration and dried at 45°C to afford **6c** (5g, 13 mmol, 95%); LCMS: Method 2; Rt 0.68 min; m/z $[M+H]^+$ 380/381.

6c (6.31 g, 16.63 mmol), 2-(2, 2-dimethylpyrrolidin-1-yl)ethanamine (2.84 g, 19.96 mmol) and triethylamine (6.96 mL, 49.9 mmol) in DMF (36.9 mL) and EtOAc (2 mL) was treated dropwise with propylphosphonic anhydride (T3P) (50% w/w in EtOAc) (15.88 g, 24.95 mmol). The resulting mixture was stirred at RT for 16 h and diluted with 10% MeOH/EtOAc (62.7 mL). The mixture was washed with 0.5M LiCl, H_2O and sat. aq. $NaHCO_3$. The aqueous layer was back-extracted with 10% MeOH: EtOAc (3 x 100 mL). The combined organic extracts was dried $MgSO_4$, filtered and concentrated *in vacuo*. The resulting solid was triturated with EtOAc and dried at 45°C. Further purification was carried out by loading the product onto 2 pre-washed 10g Isolute SCX-2 columns and washing through with MeOH. The product was eluted with 2N NH_3 in MeOH to afford a brown solid which was triturated with EtOAc to afford **22** (3.0g, 6 mmol, 36%); mp 131.3^{o}C; LCMS Method 1; Rt. 1.93 min; $[MH]^+$ m/z 504.3; purity 99%; ^{1}H NMR (400MHz, CD_3OD) δ 9.4 (1H, d), 8.45 (1H, s), 8.3 (1H, m), 8.2 (1H, s), 8.0 (1H, s), 7.85 (1H, s), 7.8 (1H, m), 7.4 (1H, m), 7.3 (1H, t), 4.0 (3H, s), 3.5 (2H, m), 2.9 (2H, t), 2.7 (2H, t), 1.8 (2H, m),

1.7 (2H, m), 1.0 (6H, s). ^{13}C NMR (D6-DMSO, 100 MHz) 164.6, 158.2, 155.7, 147.7, 138.4, 136.4, 129.6, 126.7, 126.1, 125.3, 124.6, 119.1, 117.0, 116.6, 115.4, 112.0, 110.0, 68.44, 49.8, 46.9, 38.2, 36.1, 35.0, 21.9, 18.8, 18.7; HRMS (ESI): m/z (MH^+) 504.2520. Calcd. 504.2523.

N-(2-fluoro-5-(2-(4-methylpiperazin-1-yl)benzylcarbamoyl)phenyl)-6-(1-methyl-1H-pyrazol-5-yl)pyrazolo[1, 5-a]pyridine-3-carboxamide 23; was prepared from **7d** in a similar manner to **8**. LCMS Method 1; Rt. 1.91 min; $[MH]^+$ m/z 553.2; purity >99%. ^{1}H NMR (400MHz, DMSO-d6) δ 10.0 (1H, s), 9.9 (1H, m), 9.1 (1H, s), 9.0 (1H, t), 8.9 (1H, s), 8.3 (2H, m), 7.8 (1H, m), 7.7 (1H, d), 7.55 (1H, s), 7.4 (1H, t), 7.3 (2H, m), 7.2 (2H, m), 6.6 (1H, s), 4.6 (2H, d), 4.0 (3H, s), 3.6-3.0 (8H, m), 2.9 (3H, d).^{13}C NMR(D6-DMSO, 100 MHz) 165.7, 161.4, 158.9, 156.4, 150.5, 143.3, 140.0, 138.8, 138.6, 134.1, 131.2, 129.0, 128.7, 128.3, 128.0, 126.1, 126.0, 124.3, 120.0, 119.0, 117.8, 116.3, 107.4, 106.6, 54.8, 54.8, 51.2, 51.2, 46.6, 39.3, 38.0; HRMS (ESI): m/z (MH^+) 567.2643. Calcd. 567.2632.

6-(1-Methyl-1H-pyrazol-5-yl)-N-(2-methyl-5-(2-(4-methylpiperazin-1-yl)benzylcarbamoyl) -3-yl)pyrazolo[1, 5-a]pyridine-3-carboxamide 24; was prepared from **6d** in a similar manner to **19** as a hydrochloride salt. LCMS Method 1; Rt. 1.71 min; $[MH]^+$ m/z 564.3; purity >99%. ^{1}H NMR (500MHz, DMSO-d6) δ 10.76-10.49 (1H, m), 10.16-10.05 (1H, m), 9.19 (1H, m), 9.13 (1H, m), 8.93 (1H, s), 8.89 (1H, s), 8.37 (1H, m), 8.29 (1H, d), 7.71 (1H, dd), 7.54 (1H, 2), 7.34-7.14 (4H, m), 6.59 (1H, d), 4.62 (2H, d), 3.94 (3H, s), 3.49-3.12 (8H, m), 2.84 (3H, d), 2.57(3H, s). ^{13}C NMR(D6-DMSO, 100 MHz) 163.0, 159.5, 154.8, 147.6, 142.8, 141.2, 137.8, 136.7, 136.4, 132.2, 130.9, 130.5, 126.9, 126.6, 126.3, 126.2, 122.8, 122.6, 118.2, 116.9, 115.7, 105.3, 104.6, 51.4, 51.4, 47.5, 47.5, 40.5, 36.6, 35.9, 19.6; HRMS (ESI): m/z (MH^+) 567.2643. Calcd. 564.2835.

N-(5-(2-(2, 2-dimethylpyrrolidin-1-yl)ethylcarbamoyl)-2-methylpyridin-3-yl)-6-(1-methyl-1H-pyrazol-4-yl)pyrazolo[1, 5-a]pyridine-3-carboxamide 25 was prepared from **6e** in a similar manner to **19** as the hydrochloride salt M.P.= 173^{o}C. LCMS Method 1; Rt. 1.73 min; $[MH]^+$ m/z 501.3; purity >98.2% ^{1}H NMR (400 MHz, DMSO) δ 9.75 (1H, s), 9.15 (1H, s), 8.75 (2H, m), 8.58 (1H, t), 8.32 (1H, s),

8.25 (1H, s), 8.21 (1H, d), 8.07 (1H, s), 7.82 (1H, d), 3.89 (3H, s), 3.34 (4H, m), 2.76 (2H, t), 2.56 (3H, s), 1.69 (2H, m), 1.53 (2H, m) 0.92 (6H, s). ^{13}C NMR(MeOH-D4), 100 MHz) 164.7, 163.4, 153.7, 143.7, 140.9, 139.5, 139.3, 137.6, 137.5, 131.7, 129.8, 128.4, 125.9, 122.3, 120.0, 119.5, 106.5, 71.5, 52.3, 48.6, 39.4, 38.4, 37.4, 23.6, 20.6, 20.2, 18.5. ; HRMS (ESI): m/z (MH^+) 567.2720. Calcd. 501.2726.

Supporting information.

Experimental procedures for Cell based assay/Occupancy assay; statistical test details; in vitro: in vivo correlation data(CSV); Molecular formula strings (CSV)

This material is available free of charge via the Internet at http://pubs.acs.org.

AUTHOR INFORMATION

Corresponding Author

*To whom correspondence should be addressed Duncan Shaw: Telephone :+1 6178717739; e-mail duncan.shaw@novartis.com;

IK, CT and AP were responsible for the development and execution of the PD model. FB and RS were responsible for the accompanying PK data

ACKNOWLEDGEMENTS

The authors acknowledge Caroline Marshall and Dean Moreton for performing inhalation powder delivery, Danuta Lubika for DSC melting point determinations, Benjamin Lowe for molecular modelling support, Kerry O'Hare for CHI-IAM, RSA and HSA determination.

ABBREVIATIONS

CACO2, human colon carcinoma cell; CHI-IAM, Chromatographic Hydrophobicity Index obtained from Artificial Immobilized Membrane; cKIT, CD117 receptor tyrosine kinase; CL_{INT}, Intrinsic Clearance;

D5W, 5% Dextrose in water; HATU, 1-[Bis(dimethylamino)methylene]-1H-1,2,3-triazolo[4,5-b]pyridinium 3-oxid hexafluorophosphate; ivivc, in vitro: in vivo correlation; MCT, Monocrotaline; PAH, Pulmonary Arterial Hypertension; PASMC Pulmonary Arterial Smooth Muscle cells; PDGF, Platelet Derived Growth Factor; PDGFR, Platelet Derived Growth Factor Receptor; PVR, Pulmonary Vascular Resistance; RLM, Rat Liver Microsomes; RSA, Rat Serum Albumin; SRC, sarcoma receptor tyrosine kinase; V_{ss}, Volume of distribution at steady state; SQD, Single Quadrupole Detection; TBD, 1,5,7-Triazabicyclo[4.4.0]dec-5-ene;

REFERENCES

(1) Ghofrani, H.A.; Wilkins, M.W. and Rich, S. Uncertainties in the diagnosis and treatment of pulmonary arterial hypertension. *Circulation* **2008**;*118*, 1195–1201.

(2) Badesch, D. B.; Champion, H. C.; Gomez Sanchez, M. A.; Hoeper, M.M.; Loyd, J.E.; Manes, A.; McGoon, M.; Naeige, R.; Olschewski, H.; Oudiz, R. J. and Torbicki A. Diagnosis and assessment of pulmonary arterial hypertension. *J. Am. Coll. Cardiol.* **2009**, *54*, 55S–66S.

(3) Corris, P. and Degano, B Severe pulmonary arterial hypertension: treatment options and the bridge to transplantation *Eur. Respir. Rev.* **2014**, *23*, 488–497.

(4) Perros, F.; Montani, D.; Dorfmuller, P.; Durand-Gasselin, I.; Tcherakian, C.; Le Pavec, J.; Mazmanian, M.; Fadel, E; Mussot, S.; Mercier, O.; Hervé, P.; Emilie, D.; Eddahibi, S.; Simonneau, G.; Souza, R. and Humbert, M. Platelet-derived growth factor expression and function in idiopathic pulmonary arterial hypertension. *Am. J. Respir. Crit. Care Med.*, **2008** , *178*, 81–88.

(5) Ghofrani, A.; Morrell, N. W.; Hoeper, M. M.; Olschewski, H.; Peacock, A. J.; Barst, R. J.; Shapiro, S.; Golpon, H.; Toshner, M.; Grimminger, F. and Pascoe, S Imatinib in pulmonary arterial hypertension patients with inadequate response to established therapy *Am. J. Respir. Crit. Care Med.* **2010** , *182*, 1171-1177.

(6) Frost, A. E.; Barst, R. J.; Hoeper, M. M.;Chang, H-J.; Frantz, R. P.; Fukumoto, Y.; Nazzareno, G. N.; Hassoun, P. M.; Klose, H.; Matsubara, H.; Morrell, N. W.; Peacock, A. J.; Pfeifer, M.; Simonneau, G.; Tapson, V. F.; Torres, F.; DarioVizza, C.; Lawrence, D.; Yang,W.; Felser, J. M.; Quinn, D. and Ghofrani, Long-term safety and efficacy of imatinib in pulmonary arterial hypertension *J. Heart. Lung. Transplant.***2015**, *34*, 1366-1375.

(7). A) Cooper, E. A.; Ferguson, D. and Grime, K.; Optimisation of DMPK by the inhaled route: challenges and approaches. Current Drug Metabolism, 2012, 4, 457-473. B) Tronde, A.; Norden, B.; Marchner, H.; Wendel, A.; Lennernäs, H.; Bengtsson, U. Pulmonary absorption rate and bioavailability of drugs in vivo in rats: structure-absorption relationships and physicochemical profiling of inhaled drugs. J. Pharm.Sci., **2003**, *92*, 1216-1233.

(8) Cazzola, M.; Page, C. P.; Calzetta, L and Matera, M. G. Pharmacology and therapeutics of bronchodilators. Pharmacological Reviews **2012**, *64*, 450-504

(9) Mol, C.D.; Dougan, D.R.; Schneider, T.R.; Skene, R.J.; Kraus, M.L.; Scheibe, D.N.; Snell, G.P.; Zou, H.; Sang, B.C.; Wilson, K.P. Structural basis for the autoinhibition and STI-571 inhibition of c-Kit tyrosine kinase. *J.Biol.Chem.* **2004**, *279*, 31655-31663.

(10) Bruce, I.; Chamoin, S.; Collingwood, S. P.; Furet, P.; Furminger, V.; Lewis, S.; Loren, J. C.; Molteni, V.; Saunders, A. M.; Shaw, D.; Sviridenko, L.; Thomson, C.; Yeh, V.; Janus, D.; West. R. Bicyclic heterocycle derivatives for the treatment of pulmonary arterial hypertension. PCT Int. Appl. (2013), WO 2013030802

(11) Average of N=3 test occasions. The effect of the test compound on the phosphorylation of a probe peptide substrate by PDGFRα was measured via Capillary Electrophoresis on a Caliper Labchip 3000 machine. The measurements could be used to determine an IC_{50} in a high throughput manner

(12) Average of N=3 test occasions. For full procedure refer to the supplementary information

(13) %Transcellular readings from the PAMPA assay were used as an increased resolution was seen at very low permeability rates by using this parameter

(14) DeSimone, R.W.; Currie, K.S.; Mitchell, S.A.; Darrow, J.W. and Pippin, D.A. Privileged structures: applications in drug discovery. *Comb, Chem, High Throughput Screen* **2004**, *7*:473–494.

(15) Valko, K.; Du, C.M.; Bevan, C.D.; Reynolds, D.P. and Abraham, M.H. Rapid-gradient HPLC method for measuring drug interactions with immobilized artificial membrane: comparison with other lipophilicity measures *J. Pharm. Sci.***2000**, *89*, 1085-1096.

(16) a) Mallik, R.; Yoo, M. J.; Briscoe, C. J. and Hage, D. S. Analysis of drug-protein binding by ultra fast affinity chromatography using immobilized human serum albumin. *J. Chromatogr. A.* **2010**, *1217*, 2796–2803.

b) Reilly, J.; Etheridge, D.; Everatt, B.; Jiang, Z.; Springer, C.and Fairhurst, R. A. Studies in drug albumin binding using HSA and RSA affinity methods. *J. Liq. Chromatogr. Relat. Technol.* (**2011**) ,34, 317–327.

(17) Details of Occupancy assay are in the Supplementary information

(18) Database of *in vitro* and *in silico* properties of the compounds tesed *in vivo* is part of the supplementary material

(19) Supplied by Cell Signaling Technology (www.cellsignal.com)

(20) Hollósy, F.;Valkó, K.; Hersey, A.; Nunhuck, S.; Kéri, G. and Bevan, C. Estimation of volume of distribution in humans from high throughput HPLC-based measurements of human serum albumin binding and immobilized artificial membrane partitioning. *J. Med. Chem.* **2006**, *49*, 6958-71.

(21) a) Jones, J.E.; Mendes, L.; Rudd, M.A.; Russo, G.; Loscalzo, J. and Zhang, Y-Y. Serial noninvasive assessment of progressive pulmonary hypertension in a rat model. *Am. J. Physiol. Heart Circ. Physiol.* **2002**; *283*, H364–H371.

b) Gomez-Arroyo, J.G.; Farkas, L.; Alhussaini, A.A.; Farkas, D.; Kraskauskas, D.; Voelkel, N. F. and Bogaard, H. J. The monocrotaline model of pulmonary hypertension in perspective. *Am. J. Physiol. Lung Cell Mol. Physiol.* **2012**, *302*, L363–L369

c) Stenmark, K. R.; Meyrick, B.; Galie, N.; Mooi, W. J. and McMurtry I. F. Animal models of pulmonary arterial hypertension: the hope for etiological discovery and pharmacological cure. *Am. J. Physiol. Lung Cell Mol. Physiol.* **2009**; *297*, L1013–L1032.

(22) Bruce, I.; Chamoin, S.; Furet, P.; Furminger, V.; Lewis, S.; Loren, J.; Lin L. V.; ,Molteni, V.; Saunders A. M.; Shaw, D. E.; Turner, R. and Yeh, V. 2014 WO2014132220 A1

(23) Fabian, M. A.; Biggs W. H.; Treiber D.K.; Atteridge C. E.; Azimioara M. D.; Benedetti M. G.; Carter T. A.; Ciceri P.; Edeen P. T.; Floyd M.; Ford J. M.; Galvin M, Gerlach J. L.; Grotzfeld R. M.; Herrgard S.; Insko D. E.; Insko M. A.; Lai A. G.; Lelias J. M.; Mehta S. A.; Milanov Z. V.; Velasco A. M.; Wodicka L. M.; Patel H. K.; Zarrinkar P. P. and Lockhart D. J. A small molecule-kinase interaction map for clinical kinase inhibitors. *Nat. Biotechnol*. **2005**, *3*, 329-36.

For table of contents only: